Machining of aluminium-based metal matrix composite – a particle swarm optimisation approach

Diptikanta Das*, Vivek Chakraborty, Bijaya Bijeta Nayak and Mantra Prasad Satpathy

School of Mechanical Engineering,
KIIT Deemed to be University,
Bhubaneswar-751024, Odisha, India
Email: diptikantadas@yahoo.co.in
Email: vivek_bivek@yahoo.in
Email: bijeta.mechanical@gmail.com
Email: mantraofficial@gmail.com
*Corresponding author

Chandrika Samal

Department of Mechanical Engineering,
GITA,
Bhubaneswar-752054, Odisha, India
Email: csamal100@gmail.com

Abstract: Machining performance of 5 wt.% silicon carbide particulate reinforced Al 7075 matrix composite was investigated in terms of cutting tool temperature (T), average surface roughness (Ra) and tool flank wear (VBc) during turning in pollution-free air water spray cooling environment. Metal was removed by multiple layers of TiN coated carbide inserts during turning. Nonlinear regression models were developed and their adequacies were verified. Significance of process parameters on the responses was investigated through analysis of variance. The responses were optimized individually using Taguchi technique and then simultaneously through particle swarm optimisation technique. The proposed multi-objective algorithm outperformed the traditional Taguchi approach and effectively resulted to a group of non-dominated solutions. Pareto optimal fronts were compiled and plotted for T, Ra and VBc, which can be selected according to the production requirements.

Keywords: metal matrix composite; MMC; turning; regression; analysis of variance; particle swarm optimisation.

Reference to this paper should be made as follows: Das, D., Chakraborty, V., Nayak, B.B., Satpathy, M.P. and Samal, C. (2020) 'Machining of aluminium-based metal matrix composite – a particle swarm optimisation approach', *Int. J. Machining and Machinability of Materials*, Vol. 22, No. 1, pp.79–97.

Biographical notes: Diptikanta Das is working as an Assistant Professor at the School of Mechanical Engineering, KIIT Deemed to be University, Bhubaneswar, India. He has 19 years of experience in teaching and research. His areas of research include composite fabrication and characterisation, machining of composites and hard materials, multi-criteria decision making, optimisation and simulation.

Vivek Chakraborty has completed his MTech from KIIT Deemed to be University, Bhubaneswar in 2017. His areas of research include composite fabrication and characterisation, machining of composite materials, optimisation and simulation.

Bijaya Bijeta Nayak has completed her PhD from National Institute of Technology, Rourkela, India in 2016. Currently, she is working as an Assistant Professor at the School of Mechanical Engineering, KIIT Deemed to be University, Bhubaneswar, India. Her areas of research include non-conventional machining processes and optimisation of responses.

Mantra Prasad Satpathy has completed PhD from National Institute of Technology, Rourkela, India in 2017. Currently, he is working as an Assistant Professor in School of Mechanical Engineering, KIIT Deemed to be University, Bhubaneswar, India. His areas of research include advance manufacturing process and optimisation techniques.

Chandrika Samal has completed her MTech from BPUT, Rourkela in 2010. Currently, she is working as an Assistant Professor at the Department of Mechanical Engineering, GITA, Bhubaneswar, India. Her areas of research include heat power engineering, multi-criteria decision making and optimisation of responses.

1 Introduction

Application of discontinuous silicon carbide particulate (SiC_p) reinforced Al-based metal matrix composites (MMCs) is emphasised in aircraft, naval and automotive industries, for their excellent stiffness, strength and superior resistance to wear, corrosion and thermal shock (Davim and Baptista, 2000; Davim, 2002, 2007; Mishra et al., 2015; Bains et al., 2016; Hiremath et al., 2016; Balachandar et al., 2018). But existence of hard, brittle and abrasive reinforcement particles induces machining difficulty leading to imperfection in surface finish, high rate of cutting tool wear and more cutting force requirements (Davim and Baptista, 2000; Davim, 2002; Schubert and Nestler, 2011; Radhika et al., 2014; Das et al., 2018).

While investigating machinability of SiC_p reinforced T6 conditioned Al 356 composites with poly-crystalline diamond (PCD) inserts (during turning and drilling), Davim and Baptista (2000) reported wear on the flank surface was predominant; however, crater wear was not observed. The principal wear mechanism was abrasion, and occasional adhesions were also observed. The cutting forces increased slowly with the time of machining. Davim (2002), while turning T6 conditioned Al 356/SiC_p MMC observed that the PCD inserts were more wear resistant than the chemical vapour deposited (CVD) diamond inserts. The surface finish deteriorated on reducing the cutting speed. At moderate turning parameters, the PCD inserts performed well with respect to

tool life and machined surface quality. While turning pure Al/5 wt.% SiC_p MMCs with uncoated and TiN coated carbide tools in dry condition, Kilickap et al. (2005) reported lower tool wear rate and better surface finish with the TiN coated inserts. Moreover, the tool wear increased on increasing the feed and speed of cutting; but the cutting depth was not influential for tool wear. Surface roughness reduced while turning the MMCs at higher levels of cutting speed and lower levels of feed. Lower values of tool wear were observed by Ding et al. (2005) while turning SiC_p reinforced aluminium matrix composites (AMCs) with PCD inserts as compared with poly-crystalline cubic boron nitride (PCBN) inserts, both in dry and wet machining environments. Use of coolant increased abrasion between the cutting tool and machined surface, which accelerated the groove wear and the surface quality, was deteriorated. While machining heat treated Al 356/SiC_p MMC with K10 grade tool, Davim (2007) reported that the angle of shear decreased and strain rate increased slightly on increasing the chip compression ratio. On increasing cutting velocity, strain rate increased, but the shear strain and chip compression ratio decreased. Normal stress values were higher than the shear stresses; and on increasing the feed rate, both the stresses reduced.

Flank wear of TiN coated carbide inserts increased on increasing the speed of cutting and feed rate, during turning $AlSi_7Mg_2/SiC_p$ MMC in dry condition (Ozben et al., 2008). Kannan and Kishawy (2008), while turning Al 356/SiC_p MMCs with coated carbide inserts in dry and wet cutting environments, reported very slow progression of flank wear and there was not any influence of thermal effects on the flank wear mechanism at lower levels of cutting speed (up to 120 m/min). On application of coolant, flank wear reduced remarkably even at higher levels of cutting speed, which was due to the cooling effect produced during wet turning. However, the average roughness values of the machined surfaces were more in case of wet turning.

Ultra-precision turning of as-cast Al 2024/SiC_p MMCs and extruded ZL101A/SiC_p MMCs produces many surface defects; like pits, voids, micro-cracks, grooves, protuberances and matrix tearing. The defects are caused due to pull-out and crushing of the SiC particles ahead of the cutting edge. The machined surface quality deteriorates on increasing the feed rate or by using the MMCs with higher reinforcement content (Ge et al., 2008). Ge et al. (2010) observed micro-wear, chipping, cleavage, abrasion wear and chemical wear on the single crystal diamond (SCD) tools while turning Al 2009/SiC_p MMCs in wet condition. However, during turning with PCD inserts, abrasion wear observed on the rake surface and adhesion wear observed on the flank surface. During turning of SiC_p reinforced Al 6061 composites with TiN coated carbide inserts, average surface roughness reduced at higher levels cutting speed and lower levels of feed; however, the tool flank wear accelerated at higher levels cutting speed and feed (Sahoo et al., 2013). While turning Al-Cu-TiC hybrid MMC in dry condition, Kumar et al. (2014) achieved better surface quality at higher levels of cutting speed, lower levels of feed rate and lower levels of cutting depth. In our previous work (Mishra et al., 2015), while turning 20 wt.% SiC_p reinforced Al 7075 matrix composite (in as cast condition) with uncoated carbide inserts under dry and spray cooling machining environments, it was reported that turning the composite under spray cooling environment produced machined surfaces of better quality, lower values of cutting tool temperature and higher rate of production (material removal rate). Results of grey relational analysis revealed that 0.2 mm of depth of cut, 0.04 mm/rev of feed, 930 rpm of spindle speed and 1.5 bar of air pressure (at a constant water pressure of 3 bar) was the optimal combination of

machining parameters for the multiple performance criteria (i.e., average roughness of machined surface, temperature of cutting tool and rate of material removal). Hiremath et al. (2016), while machining B_4C particulate reinforced Al 6061 matrix composites (synthesised through stir casting route), reported that the cutting forces reduced on increasing the cutting speed. Better surface quality was achieved at higher cutting speeds; however, the surface roughness increased on increasing the feed and depth of cut. Use of copper nano-fluid as machining environment during turning of H13 steel with uncoated carbide insert reduced the cutting temperature, surface roughness and tool wear up to a considerable amount compared to oil lubrication (Naresh Babu et al., 2018). Fountas et al. (2018) reported Taguchi-based genetic algorithm was a suitable method to optimise surface roughness and machining time simultaneously for cutting speed and feed rate, while turning aluminium matrix composites reinforced with stainless steel flakes. Jaafar and Al-Ethari (2018) conducted finite element simulations along with response surface methodology for improving machining performance of Ti6Al4V alloy considering cutting force, surface roughness and cutting force as responses, and cutting velocity, feed rate and tool geometry as control factors. After experimental validation it was reported that the predicted responses were within a controllable error limit of 8.4%. During turning of AISI D2 steel with coated carbide and ceramic tools, Kumar et al. (2018) reported that more tool life, good stability and more economy were achieved by the ceramic tools at high cutting speed compared to coated carbide tools.

Particle swarm optimisation (PSO) is a popular and influential method to optimise the complex engineering problems. While turning AISI H13 steel with CBN inserts, Karpat and Ozel (2007) reported dynamic neighbourhood PSO was an efficient method to solve complex multiple objective optimisation problems. During an electro discharge machining process, Sahu et al. (2013) used Box-Behnken design to produce experimental data for rate of material removal, wear on the cutting tools, roughness of machined surface and circularity of machined workpiece. A multiple-response performance characteristic index (MPCI) was generated using fuzzy interface system; and then PSO was used to get the best combination of parameters for maximising the MPCI. While turning hardened 18CrMo4 steel with CBN tools (wiper geometry), Stryczek and Pytlak (2014) compared the results of optimisation through a modified PSO method and Genetic Algorithm (GA); and reported that the PSO approach was quick and highly competitive. Good diversity, convergence and a maximum range of the Pareto front were obtained through PSO. Ananth and Vinayagam (2015) applied PSO and GA to optimise the experimental results of an Indian industry; and reported that the results of PSO had a closer resemblance to the experimental results. While solving twenty eight benchmarks multiple objective flexible job shop scheduling problems through PSO, multi-objective evolutionary algorithm (MOEA) and non-dominated sorting genetic algorithm-II (NSGA-II), Singh et al. (2016) reported that the PSO outperformed MOEA and NSGA-II in four performance matrices. Mandal and Mondal (2017) used artificial neural network (ANN) and PSO techniques to model and optimise the centreless grinding operation of C40 steel for crane hook pin.

Temperature of the cutting tool (during machining), roughness of machined surface and wear on cutting tool influence both product quality and productivity adversely. Higher levels of surface irregularities deteriorate the product quality. Increase in cutting temperature and tool flank wear influence the surface quality adversely. Moreover, if the tool flank wear will be more, less material will be removed, leading to a reduction of

productivity. So it is essential to optimise these responses individually and simultaneously to improve overall performance of machining.

A handful number of literatures are available in the open source to investigate machinability of Al-based MMCs in terms of surface roughness, tool wear, cutting force and material removal rate. However, investigation of cutting tool temperature during turning heat treated MMCs in Air Water Spray Cooling (AWSC) environment is limited. Machining of MMCs is a complex process and involves diversified outcome criteria. The complexity is more pronounced while optimising multiple responses simultaneously, that warrants the need of some advanced powerful heuristic techniques. Swam intelligence is one of the methods that satisfies the need. Though PSO has been applied successfully to resolve issues related to industries (Ananth and Vinayagam, 2015; Singh et al., 2016) and machining of steels (Karpat and Ozel, 2007; Stryczek and Pytlak, 2014; Mandal and Mondal, 2017), its application on MMC machining is not appreciable till now. Particularly, optimisation of cutting temperature, surface roughness and tool wear simultaneously using multi-objective PSO in turning Al-based MMCs has not been reported in any of the studied literatures. These gaps of previous research justify the necessity of leading to the current work. This paper presents an investigation of turning performance of heat treated Al 7075/SiC_p MMC in terms of cutting tool temperature (T), average surface roughness (Ra) and cutting tool flank wear (VBc) in AWSC environment. Also, the quality performance characteristics have been optimised simultaneously, using the PSO technique to obtain the best combinations of machining parameters, which will definitely improve the product quality and its productivity.

2 Particle swarm optimisation

It is a non-deterministic computational method inspired by the behavioural patterns of bird's flocking and swarm intelligence. The system starts with a good number of random solutions, after which it searches for the optimal values by updating generations.

In PSO, every element is known as a particle and every particle proceeds towards the region of search space at a speed which is consistently modified by own experience of the particle and experience of the whole swarm. The sharing of information socially among particles of the whole population is kept up all through the search procedure, so that the particles to move search the direction of best position. Every particle shifts towards its previous best position; and also towards the best particle in the whole swarm (Eberhart et al., 2001). At the start of the algorithm the parameters are initialised; and population is arbitrarily created within the search space.

Let us assume a search space of dimension 'd' with 'n' number particles. X_i (x_{i1}, x_{i2}, …, x_{id}) and V_i (v_{i1}, v_{i2}, …, v_{id}) represent position and velocity of i^{th} particle at a particular position in the search space. A particle's own best performance in the whole swarm is called personal best (P_{best}); and its overall best performance in the whole swarm is called global best (G_{best}). Every particle proceeds towards its P_{best} and tries to change its position with respect to its current position, current velocity, distance between the current positions, P_{best} and G_{best}. The updated position (X_i^{t+1}) and updated velocity (V_i^{t+1}) of i^{th} particle at iteration $t + 1$ can be calculated by equations (1) and (2), respectively.

$$X_i^{t+1} = X_i^t + V_i^t \tag{1}$$

$$V_i^{t+1} = wV_i^t + c_1 r_1 \left(P_{best} - X_i^t\right) + c_2 r_2 \left(G_{best} - X_i^t\right) \tag{2}$$

where X_i^t and V_i^t describes the previous position and previous velocity of i^{th} particle at iteration t. c_1 is coefficient of cognitive acceleration and c_2 is coefficient of social acceleration. r_1 and r_2 are represent two random numbers which provide stochastic characteristic of the particle velocities. w is an inertia weight parameter that can be calculated according to equation (3).

$$w = w_{\max} - \frac{w_{\max} - w_{\min}}{iter_{\max}} \times iter \tag{3}$$

where $w_{\min}$ is initial weight and $w_{\max}$ is final weight, $iter$ is the current iteration number, $iter_{\max}$ is the maximum number of iterations (Natarajan et al., 2006). The multi-objective PSO used in this work is summarised as pseudo codes illustrated in Figure 1.

Figure 1 Pseudo codes of the multi-objective PSO

```
Start
Parameters such as swarm size, repository size, maximum number of iteration, w, w^damp, c2, c2
are initialised;
Position and velocity for each particle is initialised;
Objective function for each particle is evaluated;
Personal best position for each particle is located stored;
Global best position in the swarm is located stored;
For t = 1 to number of iteration
    For i = 1 to population size
        Leader is located;
        Velocity of the particles is updated by equation (1);
        Position of the particles is updated by equation (2);
        Each particle's objective function is evaluated;
        Personal best of each particle is updated;
        If new Leader = True
            Repository is updated
    end
    Inertia weight is updated by equation (3)
end
Output repository;
end
```

3 Materials and experimental procedure

Irregular SiC_p (5 wt.% and mean particle size 8.18 μm) reinforced Al 7075 matrix composite was synthesised through vortex method of stir casting process. The detailed procedure of synthesis of the MMC is described elsewhere (Mishra et al., 2015). The

MMC sample was then solution annealed at 483°C for 2 h followed by water quenching. The quenched sample was precipitation hardened at 122°C for 24 h followed by air cooling till the room temperature is reached. These set of operation is known as T6 condition of heat treatment. A Rockwell hardness tester (make: ASI, capacity: 187.5 kgf) was employed for hardness measurement of the heat treated MMC sample, and it was observed to be 91 HRB. Optical micrograph of the T6 conditioned MMC specimen is shown in Figure 2, which shows uniformity of dispersion of the SiC particles in the matrix phase.

Figure 2 Optical micrograph of the heat treated Al 7075/5 wt.% SiC_p MMC sample

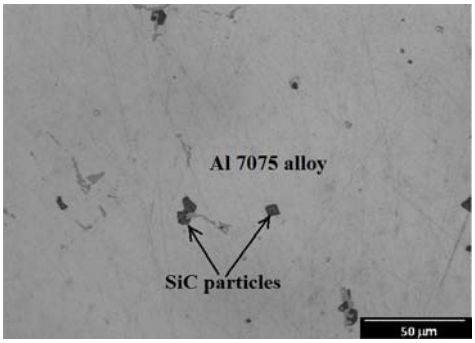

The MMC workpiece for the turning process was of dimension: 120 mm (length) × 50 mm (diameter), but the machining length was 80 mm. The machining was conducted by a high precession engine lathe (HMT-NH 22) of spindle power: 11 KW, range of spindle speed: 40–2,040 rpm in forward direction and 60–1,430 rpm in reverse direction, longitudinal feed range: 0.04–2.24 mm/rev, cross feed range: 0.02–1.12 mm/rev and tailstock sleeve travel: 200 mm. During machining, material was removed by multiple layer [TiN/TiCN/Al_2O_3/TiN] of coated tungsten carbide inserts (ISO specification: CNMG 120408), held rigidly by a turning tool holder (ISO specification: PCLNR 2525 M12). In these experiments multilayer TiN coated carbide inserts were used, as performance of these inserts are better than uncoated inserts in terms of tool wear and surface finish (Kilickap et al., 2005; Jahan et al., 2018). The machining was conducted in AWSC environment, where a mixture of compressed air (at 1.5 bar) and pressurised water (at 3 bar) was injected to the machining zone by a nozzle, at a nozzle tip distance (NTD) of 155 mm. Experimental setup during turning the MMC specimen is shown in Figure 3(a). Cutting speed, feed and depth of cut were the turning process parameters; and four levels were assigned to each parameter, as presented in Table 1. Justification of assigning four levels to the parameters was to generate more response data points for analysis and therefore the proposed optimisation process would be more adequate compared to the three level assignments. Moreover, regression models generated from the three factor-four level (3F-4L) design are more significant and more adequate than the models of three factor-three level (3F-3L) design problems, due to availability of wide response data points in the former case. Since the present study involved a 3F-4L machining problem, possible combination of parameters for experimentation was 81.

However, without going for all 81 experiments, Taguchi L_{16} orthogonal array was followed, where 16 experiments were sufficient to get an optimised parametric setting. After selecting the orthogonal array, the sequence of experiments was conducted as per the combination of levels. The quality response targets were recorded for all the experimental runs. A fresh cutting edge was used for conducting each run of the experiments.

Table 1 Turning process parameters and their levels

Turning parameters/ parametric levels	*Cutting speed, V (m/min)*	*Feed, f (mm/rev)*	*Depth of cut, d (mm)*
Level 1	40	0.05	0.2
Level 2	106	0.1	0.3
Level 3	169	0.16	0.4
Level 4	206	0.2	0.5

Figure 3 Experimental setup for (a) turning the MMC sample in AWSC environment and (b) surface roughness measurement (see online version for colours)

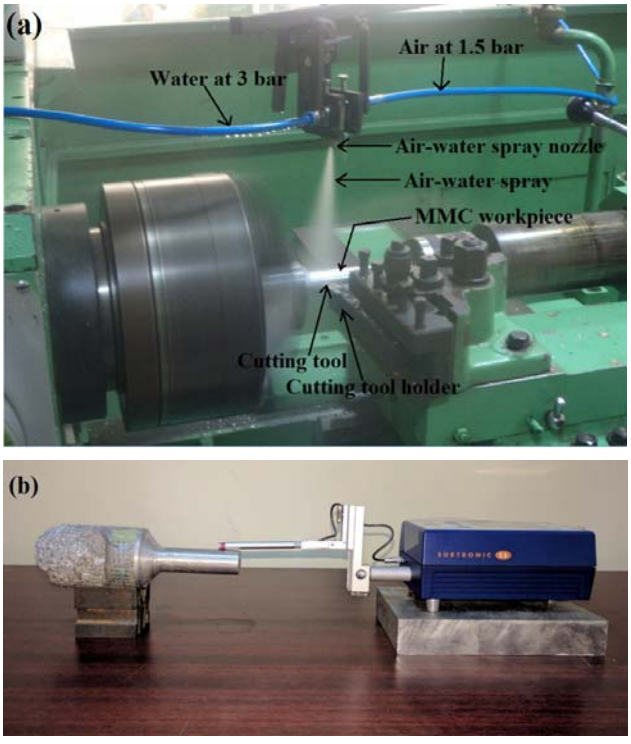

During the turning operation, cutting tool temperature (T) was measured using a self calibrating type high-definition infrared thermal imager (Fluke Ti32). The imager was hold at a distance of 200 mm from the tool and it was focused on its rake surface (close to the nose) for the temperature measurement. Temperature was measured four times for each experimental run at an interval of 20 mm machining length. Average of all the four measured data represented the tool temperature for that particular run. Arithmetic average roughness (Ra) of the machined surfaces was measured using a high precision surface roughness tester (Taylor Hobson-Surtronic 25). During surface roughness measurement, first of all the roughness tester was calibrated using a reference specimen and then the pickup stylus was positioned on the machined work surface parallel to it. Then measurement was conducted considering an assessment length of 4 mm and cut-off length of 0.8 mm. The measurement was repeated at four different places on the work surface and the average of measured data was considered for further analysis. Experimental setup for the surface roughness measurement is shown in Figure 3(b). Flank wear (VBc) of the cutting tool was measured after each run of the turning operation using Nikon-V10AD profile projector. The flank wear was measured at the nose corner as the depth of cut for each run was less than the nose radius (0.8 mm). Images of worn inserts were captured by Radical Instruments-RSM 8 stereo zoom microscope.

4 Results and discussion

4.1 Investigation on turning performance

Experimental results of T, Ra and VBc are presented in Table 2, during turning the Al 7075/5 wt.% SiC_p MMC in AWSC environment. Means of the responses (T, Ra, and VBc) were computed and their main effects plots were generated [Figures 4(a)–4(c)] through MINITAB 17 software, considering smaller is better criteria for all the responses. Experimental results (Table 2) reveal that the cutting temperature was minimum (33.8°C) at 40 m/min of cutting speed, 0.05 mm/rev of feed and 0.2 mm of cutting depth. It increased to a maximum value (79.27°C) at run 13, i.e., at highest cutting speed level (206 m/min) and at highest cutting depth level (0.5 mm). From the main effects plot for means of T [Figure 4(a)], it is evident that T increased on increasing cutting speed, feed or depth of cut. Also, the highest influencing parameter on cutting temperature was cutting speed, followed by depth of cut and feed. Increased friction and increased cutting force components (Kumar et al., 2014) at higher levels of machining parameters are the predominant causes of increase in temperature.

Average roughness of the machined surface was minimum (0.67 µm) at run 13, i.e., at the cutting speed of 206 m/min, feed of 0.05 mm/rev and depth of cut of 0.5 mm. Main effects plot for means of Ra [Figure 4(b)] reveals that Ra reduced with increasing the speed of cutting, but it increased with increasing feed. Though Ra increased with increasing the cutting depth, it had the least influence. Higher values of Ra at lower cutting speed were due to more work-tool contact area, which caused more friction. At higher machining speeds, the friction reduced due to reduction of the contact area; and therefore the surface quality improved. As the feed increases, friction between the cutting tool and work surface increases, leading to higher values of surface roughness. Moreover, on increasing the depth of cut thrust force component increases that cause vibration in the workpiece, leading to an inferior surface quality.

Table 2 Experimental results for T, Ra and VBc along with their S/N values

Run no.	*V*	*f*	*d*	*T (°C)*	*Ra (μm)*	*VBc (mm)*	*S/N of T*	*S/N of Ra*	*S/N of VBc*
1	40	0.05	0.2	33.8	0.82	0.075	–30.578	1.72372	22.49877
2	40	0.1	0.3	44.77	1.38	0.098	–33.02	–2.7976	20.17548
3	40	0.16	0.4	47.93	1.52	0.109	–33.612	–3.6369	19.25147
4	40	0.2	0.5	58.5	2.11	0.139	–35.343	–6.4856	17.1397
5	106	0.05	0.3	44.9	0.73	0.131	–33.045	2.73354	17.65457
6	106	0.1	0.2	52.5	1.02	0.148	–34.403	–0.172	16.59477
7	106	0.16	0.5	69.33	1.5	0.152	–36.818	–3.5218	16.36313
8	106	0.2	0.4	71.63	1.9	0.16	–37.102	–5.5751	15.9176
9	169	0.05	0.4	56.13	0.7	0.159	–34.984	3.09804	15.97206
10	169	0.1	0.5	67.8	1.23	0.168	–36.625	–1.7981	15.49381
11	169	0.16	0.2	60.7	1.35	0.184	–35.664	–2.6067	14.70364
12	169	0.2	0.3	68.4	1.64	0.192	–36.701	–4.2969	14.33398
13	206	0.05	0.5	79.27	0.67	0.201	–37.982	3.4785	13.93608
14	206	0.1	0.4	74.93	0.98	0.221	–37.493	0.17548	13.11215
15	206	0.16	0.3	72.93	1.25	0.241	–37.258	–1.9382	12.35966
16	206	0.2	0.2	69.7	1.59	0.248	–36.865	–4.0279	12.11097

Figure 4 Main effects plot for (a) means of T, (b) means of Ra and (c) means of VBc (see online version for colours)

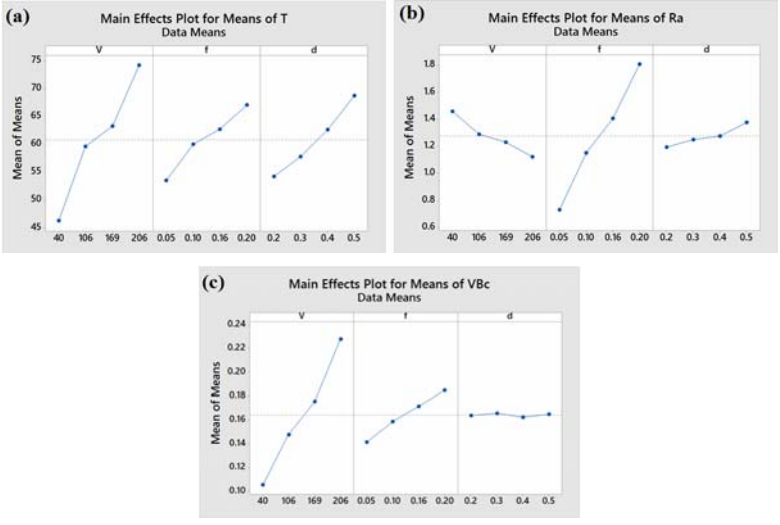

From the results of experiments (Table 2), it is revealed that the tool flank wear was minimum (0.075 mm) at the lowest levels of parameters, i.e., at 40 m/min of cutting speed, 0.05 mm/rev of feed and 0.2 mm of cutting depth. Main effects plot for means of VBc [Figure 4(c)] reveals that VBc increased on increasing the speed of cutting and feed. For VBc, cutting speed was the highest influencing parameter, taken after by feed and depth of cut. Higher flank wear values were due to more workpiece-tool friction and more cutting force components at higher levels of machining parameters. Moreover, on increasing the cutting speed or feed, the hard abrasive SiC particles hit the tool at comparatively higher speed and micro-cut its sharp cutting edge. On increasing the depth of cut, more number of SiC particulates are crushed by the cutting edge, leading to severe tool wear. However, the experimental data (Table 2) reveal that the values of flank wear were within the limiting criterion of 0.3 mm (ISO 3685:1993) for all the runs; which imply the potentiality of the multilayer TiN coated carbide inserts to machine Al-based MMCs. Images of some worn cutting tools after turning are presented in Figures 5(a)–5(c), as illustration.

Figure 5 Images of worn cutting tools after (a) run 1, (b) run 7 and (c) run 14 (see online version for colours)

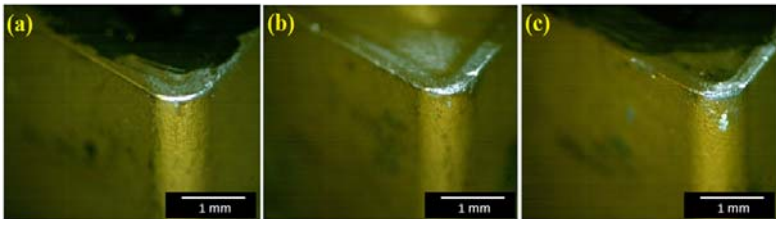

4.2 Single objective optimisation

The responses under consideration (i.e., T, Ra and VBc) were optimised individually using Signal to noise ratio (S/N) concept of Taguchi method. Considering smaller is better criteria for all the responses, the S/N were generated and presented in Table 2. Main effects plots of the individual responses were plotted through MINITAB 17 software, which are shown in Figures 6(a)–6(c) for T, Ra and VBc, respectively. From Figures 6(a) and 6(c), highest values of S/N were obtained for the parametric combinations of V_1-f_1-d_1, i.e., 40 m/min of V, 0.05 mm/rev of f and 0.2 mm of d. These were the optimal parameters for T and VBc individually. Similarly from Figure 6(b), optimal combination of parameters for Ra was V_4-f_1-d_1, i.e., 206 m/min of V, 0.05 mm/rev of f and 0.2 mm of d.

4.3 Analysis of variance

Analysis of variance (ANOVA) was conducted at 95% confidence level using adjusted sum of squares for tests to observe the significance of the machining process parameters and their percentage of contribution on the responses (T, Ra and VBc). ANOVA results of T are presented in Table 3, which reveals that cutting speed is the most significant

parameter for T (with lowest P-value), taken after by cutting depth and feed. The contribution of V, f and d for the cutting tool temperature are 62.23%, 15.04% and 18.63% respectively. For all the three parameters the statistical Fisher's constant (F) values are more than the tabulated F-value (4.76) [Panneerselvam, 2014] at 95% confidence level. It can be observed from Table 4 that the highest significant parameter for Ra is feed, taken after by cutting speed. Influence of depth of cut on Ra is not significant. Similarly, Table 5 represents the ANOVA results for VBc, which reveals that cutting speed is the highest significant process parameter (with contribution of 87.34%) for the tool flank wear, taken after by feed (with contribution of 11.26%). For VBc, the influence of depth of cut is also insignificant.

Figure 6 Main effects plot for (a) S/N of T, (b) S/N of Ra and (c) S/N of VBc (see online version for colours)

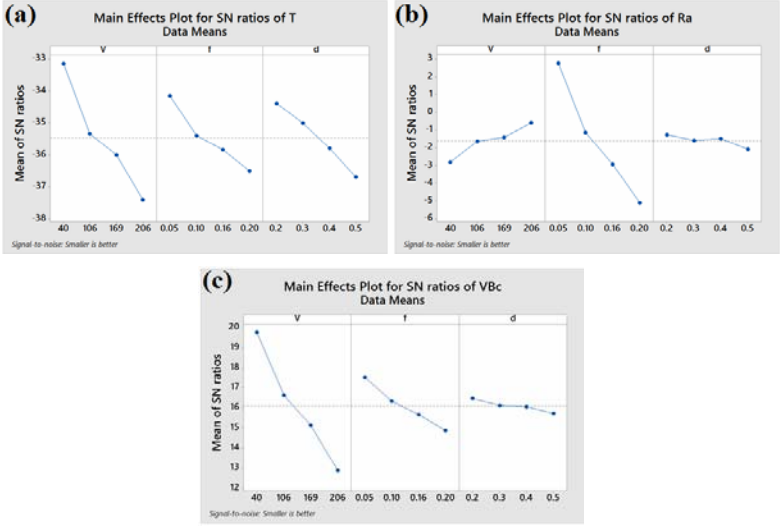

Table 3 Analysis of variance for T

Source	*Degrees of freedom*	*Sum of squares*	*Mean square*	*Fisher's constant (F)*	*Probability of significance (P)*	*% of contribution*
V	3	1595.86	531.95	30.37	0.001	62.23
f	3	385.66	128.55	7.34	0.02	15.04
d	3	477.75	159.25	9.09	0.012	18.63
Error	6	105.08	17.51			4.10
Total	15	2,564.35				100.00

Table 4 Analysis of variance for Ra

Source	*Degrees of freedom*	*Sum of squares*	*Mean square*	*Fisher's constant (F)*	*Probability of significance (P)*	*% of contribution*
V	3	0.23497	0.07832	12.6	0.01	8.38
f	3	2.46062	0.82021	131.98	0.00	87.79
d	3	0.07012	0.02337	3.76	0.08	2.50
Error	6	0.03729	0.00621			1.33
Total	15	2.80299				100.00

Table 5 Analysis of variance for VBc

Source	*Degrees of freedom*	*Sum of squares*	*Mean square*	*Fisher's constant (F)*	*Probability of significance (P)*	*% of contribution*
V	3	0.0316708	0.0105569	131.55	0.00	87.34
f	3	0.0040823	0.0013608	16.96	0.00	11.26
d	3	0.0000253	0.0000084	0.1	0.95	0.07
Error	6	0.0004815	0.0000802			1.33
Total	15	0.0362598				100.00

4.4 Regression analysis

Nonlinear regression models were developed at 95% confidence level for T, Ra and VBc by MINITAB 17 statistical software using the experimental data (un-coded units) from Table 3. The nonlinear regression equations for the objectives are presented in equations (4)–(6). The normal probability plots of residuals [Figures 7(a)–7(c)] depict normal distribution of errors; and closeness of residuals to the normal probability lines. It reveals that the predicted models are significant and adequate.

$$T = 40.4667 + 0.0182V + 191.1792f - 111.9591d - 80.1191f^2 + 63.4984d^2 - 0.6107Vd + 158.2751fd \tag{4}$$

$$Ra = 0.6218 - 0.0033V + 6.7721f - 0.0771d + 3.4689f^2 + 1.1839d^2 + 0.0019Vd - 2.7010fd \tag{5}$$

$$VBc = 0.0651 + 0.0006V + 0.0073f - 0.0653d - 0.3071f^2 + 0.0266d^2 - 0.0008Vd + 1.0736fd \tag{6}$$

4.5 Multi-objective optimisation

All the responses (i.e., T, Ra and VBc) were optimised simultaneously using multi-objective PSO algorithm, where equations (4), (5) and (6) were employed as the fitness functions. This algorithm contained very less number of tuning parameters, and it had the advantage to reach the global optimum solution at a less computational time. The algorithm parameter settings are furnished in Table 6. The multi-objective PSO resulted a

set of non-dominated solutions for all the three responses, which are presented in the Table 7.

Figure 7 Normal probability plot of residuals for (a) T, (b) Ra and (c) VBc (see online version for colours)

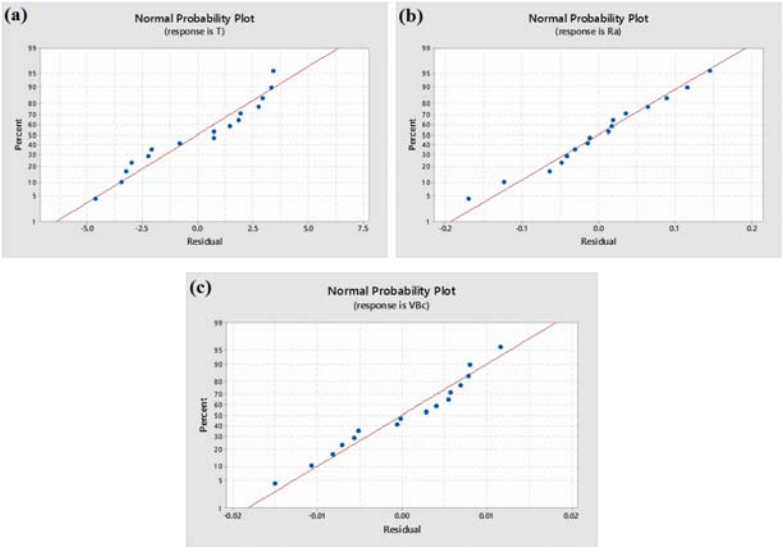

Table 6 Algorithm parameter settings for multi-objective PSO

Tuning Parameters	*Values*
Number of iterations	500
Population size	200
Repository size	30
w	1
w^{damp}	0.99
c_1	1
c_2	2

From the optimisation results, it can be inferred that at the V_1-f_1-d_3 optimal parametric condition, lowest values of T (27.158 °C) and VBc (0.076 mm) were obtained. Likewise, at V_4-f_1-d_1 optimal parametric condition, the minimum value of Ra (0.4462 µm) was observed. Furthermore, the results of traditional Taguchi philosophy and multi-objective PSO were compared, and presented in Table 8. Multi-objective PSO demonstrated better

results than the traditional Taguchi approach. Finally, some confirmation experiments were performed, which showed the errors of 2.12%, 2.76% and 3% for T, Ra and VBc, respectively between the experimental and multi-objective PSO results. Figure 8 portrays the compiled Pareto optimal front for non-dominated solutions of T, Ra and VBc, which may be selected as per production needs. The proposed multi-objective PSO is of high competitiveness to converge towards the Pareto front.

Table 7 Results of multi-objective PSO for T, Ra and VBc

Sl. no.	*V*	*f*	*d*	*T*	*Ra*	*VBc*
1	66.615	0.0500	0.2000	39.099	0.7892	0.1005
2	196.320	0.0500	0.2032	55.328	0.4699	0.2321
3	40.000	0.0501	0.3727	28.568	0.9536	0.0778
4	40.000	0.0502	0.4219	27.158	0.9934	0.0766
5	188.587	0.0501	0.2000	54.185	0.4858	0.2226
6	120.733	0.0500	0.2000	45.582	0.6486	0.1460
7	184.100	0.0500	0.2000	53.599	0.4961	0.2168
8	206.000	0.0500	0.2045	56.684	0.4487	0.2449
9	85.901	0.0500	0.2000	41.368	0.7379	0.1151
10	163.510	0.0501	0.2000	50.953	0.5447	0.1917
11	165.475	0.0501	0.2040	51.298	0.5425	0.1935
12	148.704	0.0503	0.2000	49.097	0.5815	0.1749
13	57.956	0.0500	0.2000	38.093	0.8125	0.0945
14	71.277	0.0501	0.2000	39.662	0.7774	0.1039
15	109.628	0.0500	0.2008	44.214	0.6771	0.1355
16	206.000	0.0500	0.2000	56.473	0.4462	0.2457
17	40.934	0.0500	0.2000	36.138	0.8590	0.0837
18	80.238	0.0500	0.2011	40.671	0.7535	0.1106
19	40.000	0.0500	0.3980	27.783	0.9727	0.0772
20	114.361	0.0500	0.2000	44.808	0.6650	0.1399
21	90.749	0.0500	0.2000	41.947	0.7253	0.1191
22	180.996	0.0500	0.2000	53.193	0.5030	0.2129
23	40.000	0.0500	0.2000	36.027	0.8614	0.0832
24	40.000	0.0500	0.3400	29.686	0.9307	0.0787
25	40.000	0.0501	0.2673	32.678	0.8892	0.0809
26	55.521	0.0501	0.2000	37.817	0.8193	0.0929
27	206.000	0.0500	0.2013	56.532	0.4470	0.2455
28	87.982	0.0501	0.2000	41.628	0.7330	0.1168
29	92.019	0.0500	0.2000	42.106	0.7223	0.1201
30	146.570	0.0500	0.2053	48.855	0.5876	0.1719

Table 8 Results of comparison between Taguchi philosophy and multi-objective PSO

Methods	*Optimal parametric combination*	*Responses*		
		T (°C)	*Ra (mm)*	*VBc (μm)*
Taguchi philosophy	V_1-f_1-d_1	32.29	-	0.082
	V_4-f_1-d_1	-	0.498	-
Multi-objective PSO	V_1-f_1-d_3	27.15	-	0.076
	V_4-f_1-d_1	-	0.446	-
Experimental	V_1-f_1-d_3	26.59	-	0.073
	V_4-f_1-d_1	-	0.434	-

Figure 8 Pareto front for non-dominated solutions of T, Ra and VBc (see online version for colours)

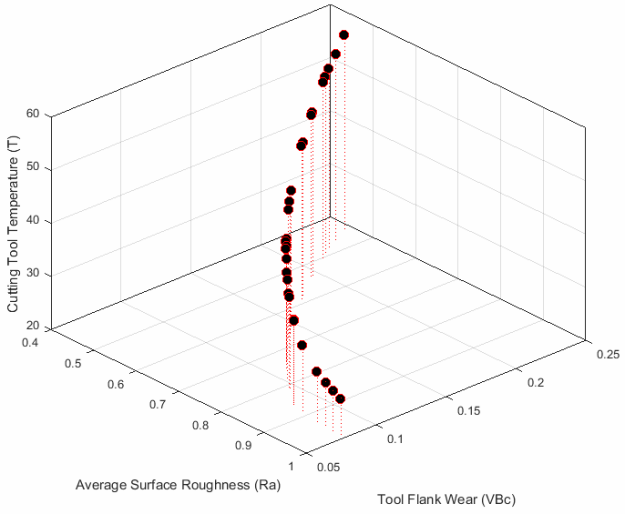

5 Conclusions

- During turning the T6 conditioned Al 7075/5 wt.% SiC_p MMC in AWSC environment, the cutting tool temperature increased on increasing any of the machining process parameters under consideration, i.e., cutting speed, feed or depth of cut. Average roughness of the machined surface reduced with increasing the speed of cutting; but with increasing feed or depth of cut, it increased. Tool flank wear increased with increasing either speed of cutting or feed or depth of cut. The flank wear values were within the limiting criterion of 0.3 mm for all the experimental runs; which revealed the potentiality of multilayer TiN coated carbide inserts to machine the Al-based MMCs.

- Results of ANOVA revealed that cutting speed (62.23% of contribution) was the most significant parameter for cutting tool temperature, taken after by depth of cut and feed. Highest significant parameter for average surface roughness was feed (87.79% of contribution), taken after by cutting speed; however, depth of cut was not significant. Similarly, for the tool flank wear, cutting speed (87.34% of contribution) was the most significant process parameter, taken after by feed; but depth of cut was not significant.
- Nonlinear regression models were developed for the responses at 95% confidence level; and their adequacies were verified through normal probability plots of residuals.
- Multi-objective PSO generated better results for the responses than those of conventional Taguchi method. It resulted to a set of non-dominated solutions successfully. Pareto optimal fronts were compiled and plotted for T, Ra and VBc; which could be selected according to production requirements. The confirmation experiments showed the errors of 2.12%, 2.76% and 3% for T, Ra and VBc respectively, while comparing the experimental and PSO results. These results indicated that this approach was exceedingly viable and can be considered as a feasible alternative to solve multiple objective optimisation problems.

References

Ananth, G. and Vinayagam, B.K. (2015) 'Effectiveness improvement through total productive maintenance using particle swarm optimisation model for small and micro manufacturing enterprises', *Int. J. Productivity and Quality Management*, Vol. 16, No. 4, pp.473–503.

Bains, P.S., Sidhu, S.S. and Payal, H.S. (2016) 'Fabrication and machining of metal matrix composites: a review', *Materials and Manufacturing Processes*, Vol. 31, No. 5, pp.553–573.

Balachandar, R., Balasundaram, R., Srinivasan, D. and Raj Kumar G. (2018) 'Cut quality characteristics of Al 6061-T6 composites using abrasive water jet machining', *Int. J. Materials Engineering Innovation*, Vol. 9, No. 3, pp.179–194.

Das, D., Mishra, P.C., Singh, S., Chaubey, A.K. and Routara B.C. (2018) 'Machining performance of aluminium matrix composite and use of WPCA based Taguchi technique for multiple response optimization', *International Journal of Industrial Engineering Computations*, Vol. 9, No. 4, pp.551–564.

Davim, J.P. (2002) 'Diamond tool performance in machining metal–matrix composites', *J. Materials Processing Technology*, Vol. 128, Nos. 1–3, pp.100–105.

Davim, J.P. (2007) 'Application of Merchant theory in machining particulate metal matrix composites', *Materials and Design*, Vol. 28, No. 10, pp.2684–2687.

Davim, J.P. and Baptista, A.M. (2000) 'Relationship between cutting force and PCD cutting tool wear in machining silicon carbide reinforced aluminium', *J. Materials Processing Technology*, Vol. 103, No. 3, pp.417–423.

Ding, X., Liew, W.Y.H. and Liu, X.D. (2005) 'Evaluation of machining performance MMC with PCBN and PCD Tools', *Wear*, Vol. 259, Nos. 7–12, pp.1225–1234.

Eberhart, R.C., Shi, Y. and Kennedy, J. (2001) *Swarm Intelligence*, Morgan Kaufmann series in evolutionary computation, Morgan Kaufmann Publishers, San Diego, USA.

Fountas, N.A., Seretis, G.V., Manolacos, D.E., Provatidis, C.G. and Vaxevanidis, N.M. (2018) 'Multi-objective statistical analysis and optimisation in turning of aluminium matrix particulate composite using genetic algorithms', *Int. J. Machining and Machinability of Materials*, Vol. 20, No. 3, pp.236–250.

Ge, Y.F., Xu, J.H. and Yang, H. (2010) 'Diamond tools wear and their applicability when ultra-precision turning of SiCp/2009Al matrix composite', *Wear*, Vol. 269, Nos. 11–12, pp.699–708.

Ge, Y.F., Xu, J.H., Yang, H., Luo, S.B. and Fu, Y.C. (2008) 'Workpiece surface quality when ultra-precision turning of SiC_p/Al composites', *J. Materials Processing Technology*, Vol. 203, pp.166–175.

Hiremath, V., Auradi, V. and Dundur, S.T. (2016) 'Machining of metal matrix composites: influence of B_4C ceramic particulate addition on cutting forces and surface roughness of 6061Al alloy', *International Journal of Machining and Machinability of Materials*, Vol. 18, No. 4, pp.365–376.

Jaafar, A.H. and Al-Ethari, H. (2018) 'Optimisation of machining TI6AL4V alloy: numerical simulation and experimental verification', *Int. J. of Machining and Machinability of Materials*, Vol. 20, No. 5, pp.447–459.

Jahan, M.P., Arbuckle, G.K. and Rumsey, A.M. (2018) 'A comparative study on the effectiveness of TiN, TiCN, and AlTiN coated carbide tools for dry micro-milling of aluminium, copper and brass at low spindle speed', *Int. J. of Machining and Machinability of Materials*, Vol. 20, No. 2, pp.141–164.

Kannan, S. and Kishawy, H.A. (2008) 'Tribological aspects of machining aluminium metal matrix composites', *J. Mater. Process. Technol.*, Vol. 198, Nos. 1–3, pp.399–406.

Karpat, Y. and Ozel, T. (2007) 'Multi-objective optimization for turning processes using neural network modeling and dynamic-neighborhood particle swarm optimization', *Int. J. Adv Manuf. Technol.*, Vol. 35, Nos. 3–4, pp.234–247.

Kilickap, E., Cakir, O., Aksoy, M., et al. (2005) 'Study of tool wear and surface roughness in machining of homogenized SiCp reinforced aluminium metal matrix composite', *J. Mater Process. Technol.*, Vol. 164, pp.862–867.

Kumar, A., Mahapatra, M.M. and Jha, P.K. (2014) 'Effect of machining parameters on cutting force and surface roughness of in situ Al-4.5%Cu/TiC metal matrix composites', *Measurement*, Vol. 48, pp.325–332.

Kumar, R., Sahoo, A.K., Mishra, P.C. and Das, R.K. (2018) 'An investigation to study the wear characteristics and comparative performance of cutting inserts during hard turning', *Int. J. of Machining and Machinability of Materials*, Vol. 20, No. 4, pp.320–344.

Mandal, P. and Mondal, S.C. (2017) 'An application of artificial neural network and particle swarm optimisation technique for modelling and optimisation of centreless grinding process', *Int. J. Productivity and Quality Management*, Vol. 20, No. 3, pp.344–362.

Mishra, P.C., Das, D.K., Ukamanal, M., Routara, B.C. and Sahoo, A.K. (2015) 'Multi-response optimization of process parameters using Taguchi method and grey relational analysis during turning AA 7075/SiC composite in dry and spray cooling environments', *Int. J. Industrial Engineering Computations*, Vol. 6, No. 4, pp.445–456.

Naresh Babu, M., Anandan, V., Muthukrishnan, N. and Gajendiran, M. (2018) 'Experimental process to evaluate the minimum quantity lubrication technique using copper nanofluids in turning process', *Int. J. Machining and Machinability of Materials*, Vol. 20, No. 6, pp.497–512.

Natarajan, U., Saravanan, R. and Periasamy, V.M. (2006) 'Application of particle swarm optimisation in artificial neural network for the prediction of tool life', *Int. J Advanced Manufacturing Technology*, Vol. 28, Nos. 11–12, pp.1084–1088.

Ozben, T., Killickap, E. and Cakir, O. (2008) 'Investigation of mechanical and machinability properties of SiC particle reinforced Al-MMC', *J. Mater. Process. Technol.*, Vol. 198, Nos. 1–3, pp.220–225.

Panneerselvam, R. (2014) *Research Methodology*, 2nd ed., PHI Learning Private Limited, India.

Radhika, N., Subramanian, R. and Sajith, A. (2014) 'Analysis of chip formation in machining aluminum hybrid composites', *E3 Journal of Scientific Research*, Vol. 2, No. 1, pp.9–15.

Sahoo, A.K., Pradhan, S. and Rout, A.K. (2013) 'Development and machinability assessment in turning Al/SiC_p-metal matrix composite with multilayer coated carbide insert using Taguchi and statistical techniques', *Archives of Civil and Mechanical Engineering*, Vol. 13, No. 1, pp.27–35.

Sahu, J., Mahapatra, S.S. and Puhan, D. (2013) 'Multi-response optimisation of electrical discharge machining process using combined approach of RSM and FIS', *Int. J. Productivity and Quality Management*, Vol. 12, No. 2, pp.185–208.

Schubert, A. and Nestler, A. (2011) 'Enhancement of surface integrity in turning of particle reinforced aluminum matrix composites by tool design', *Procedia Engineering*, Vol. 19, pp.300–305.

Singh, M.R., Singh, M., Mahapatra, M.M. and Jagadev, N. (2016) 'Particle swarm optimization algorithm embedded with maximum deviation theory for solving multi-objective flexible job shop scheduling problem', *Int. J. Advanced Manufacturing Technology*, Vol. 85, Nos. 9–12, pp.2353–2366.

Stryczek, R. and Pytlak, B. (2014) 'Multi-objective optimization with adjusted PSO method on example of cutting process of hardened 18CrMo4 steel', *Maintenance and Reliability*, Vol. 16, No. 2, pp.236–245.